Available at www.sciencedirect.com

ScienceDirect

journal homepage: www.elsevier.com/locate/he

The catalytic reforming of bio-ethanol over SiO_2 supported ZnO catalysts: The role of ZnO loading and the steam reforming of acetaldehyde

*Erol Seker**

Chemical Engineering Department, Izmir Institute of Technology, Gulbahce Campus, Urla, Izmir 35430, Turkey

ARTICLE INFO

Article history:
Received 23 June 2007
Received in revised form
7 November 2007
Accepted 15 February 2008

Keywords:
Ethanol
Zinc oxide
Acetone
Acetaldehyde
Propene
Steam reforming

ABSTRACT

In this study, the activity and the product distributions of sol–gel made SiO_2 supported ZnO catalysts in the steam reforming of ethanol and acetaldehyde is presented as a function of ZnO loading and temperature. We show that although highly dispersed ZnO in SiO_2 (upto 50% ZnO loading) can be prepared using a single step sol–gel method, a precise control of crystallite size could not be achieved. From CO_2 TPD measurements, we found that the basic site densities of ZnO/SiO_2 catalysts stays $<0.05\,\mu mol/m^2$ and do not increase linearly with ZnO loading. The highest basic site density among the catalysts occurs on pure ZnO.

All ZnO/SiO_2 catalysts are active at 350 °C whereas pure ZnO catalyst is active at 450 °C. Iso-conversion activity tests show that ethanol steam reforming activities of the catalysts seem to be dependent on the ZnO crystallite size rather than the basic site density of the catalysts when the surface coverage of the basic site density is <0.32% but acetone is not formed only on catalysts with ZnO crystallite size <5 nm regardless of their basic site densities. Interestingly, we found that ethanol was mostly dehydrogenated to acetaldehyde and hydrogen although H_2O/C_2H_5OH molar ratio in the feed was 12. CO was not also produced in the steam reforming of ethanol over all the catalysts. Acetone and propene are produced from acetaldehyde as observed in the steam reforming of acetaldehyde. The steam reforming of acetaldehyde as compared to its decomposition was found to be more favorable over the catalysts with small ZnO crystals, such as 30% and 50% ZnO catalysts.

1. Introduction

Efforts to reduce the emission of toxic and green house gases, such as NO_x and CO_2, and also to lower the high consumption rates of the fossil fuel reserves have generated considerable interests in using alternative technologies, such as fuel cells, and/or alternative fuels, such as bio-alcohols, natural gas, hydrogen and biodiesel [1–3]. Among alternative fuels, hydrogen seems to be a viable energy carrier for future. Unfortunately, it is not freely available in nature and it must be produced by some means. Most importantly, the hydrogen fuel infrastructure is not available currently. Hence, these obstacles have forced the research efforts to focus on developing novel catalysts for the catalytic hydrogen production from hydrocarbons and alcohols, such as gasoline and methanol [4–6]. Although methanol and hydrocarbons seem to be good candidates for hydrogen production, carbon dioxide emission is still the problem because methanol and

*Tel.: +90 232 750 6646; fax: +90 232 750 6645.
E-mail address: erolseker@iyte.edu.tr
0360-3199/$ - see front matter © 2008 International Association for Hydrogen Energy. Published by Elsevier Ltd. All rights reserved.
doi:10.1016/j.ijhydene.2008.02.033

hydrocarbons are obtained from fossil fuels. In contrast, the use of bio-ethanol to produce hydrogen could release carbon dioxide which is used by new crops to grow; hence resulting in a net zero carbon dioxide emission. Although ethanol seems to be a promising fuel to produce hydrogen, the studies on the reforming of ethanol to produce hydrogen are less than that on methanol and hydrocarbons.

Thermodynamic analyses have shown that a high conversion of ethanol to hydrogen is possible above 250°C and also the high water/ethanol molar ratio is beneficial to increase hydrogen yield and to decrease the formation of by-products, such as methane and carbon monoxide, and carbon deposition. The steam reforming of ethanol occurs through the following possible network of reactions [7–9]:

$$C_2H_5OH + H_2O \rightarrow 2CO + 4H_2$$
(reforming of ethanol) (1)

$$CO + H_2O \leftrightarrow CO_2 + H_2$$
(water gas shift reaction) (2)

$$C_2H_5OH \rightarrow C_2H_4 + H_2O$$
(dehydration of ethanol) (3)

$$C_2H_5OH \rightarrow C_2H_4O + H_2$$
(dehydrogenation of ethanol) (4)

$$C_2H_4O + H_2O \rightarrow 2CO + 3H_2$$
(steam reforming of acetaldehyde) (5)

$$CO + 3H_2 \leftrightarrow CH_4 + H_2O$$
(methanation reaction) (6)

A catalyst under certain reaction conditions favors a reaction or a group of the reactions among a possible network of reactions shown above. It is known that acidic catalysts, such as alumina, enhance the dehydration reaction whereas basic catalysts, such as magnesium oxide, increase the rate of dehydrogenation reaction [10,11]. Fumihiro et al. [12] reported that the activity and the product distribution of supported cobalt catalysts were strongly dependent on the support material and found out that among Al_2O_3, ZrO_2, MgO, SiO_2 and carbon support materials, Al_2O_3 used to support cobalt was the most active and selective to hydrogen. Also, alumina supported rhodium and nickel catalysts and lanthana promoted Ni/γ-Al_2O_3 catalysts were found to be active and selective to hydrogen in the bio-ethanol steam reforming over 600 °C and their activities depended on the metal loading [13–15]. Besides, many transition metals (ranging from gold to platinum group metals to base metals) supported on oxides, such as ceria, lanthana and zirconia, were also investigated in the steam reforming of ethanol. For instance, Zhang et al. [16] reported that ceria supported Co, Ir and Ni catalysts were active and selective to hydrogen in the temperature range from 300 to 700°C. Similarly, oxide supported bimetallic catalysts, aluminum spinels and also some commercially available catalysts were found to be active and selective to hydrogen at high temperatures for the bio-ethanol steam reforming [17–19]. Among the catalysts studied up until now, ZnO based catalysts seem to be promising. Llorca et al. [20] was the first group to show that pure ZnO among the oxides, such as alumina, magnesia, ceria and titania, was the most active at low temperatures (~400 °C) to produce hydrogen from bio-ethanol. Later, Llorca et al. [21] reported that the addition of cobalt to ZnO further improved the activity at low temperatures in the steam reforming of ethanol. Similarly, Yang et al. [22] recently reported that Ni/ZnO, Ni/La_2O_3, Ni/MgO and Ni/Al_2O_3 catalysts were highly active (100% ethanol conversion) at temperatures ranging from 330 to 650 °C but the product distribution was strongly dependent on the support material and the nickel loading. It is difficult to make a sound comparison between results reported by research laboratories around the world because there are differences in the feed conditions, space velocities and the reactor setup configuration used to test the catalytic activity and selectivity.

In this manuscript, the effect of zinc oxide loading on the catalytic activity and the product selectivity in the catalytic reforming of bio-ethanol are reported for ZnO supported on silica catalysts (ZnO/SiO_2), and also pure ZnO and pure SiO_2 catalysts. In addition, acetaldehyde steam reforming was studied over ZnO/SiO_2 catalysts and pure ZnO to better understand the role of acetaldehyde on the product distribution during the catalytic reforming of bio-ethanol.

2. Experimental

2.1. *Catalyst preparation*

ZnO/SiO_2 catalysts with 30, 50 and 70 wt% of ZnO loadings (chosen based on our previous unpublished results) and pure SiO_2 were synthesized using a single step sol–gel approach and also, pure ZnO catalyst was prepared using the precipitation method.

The sol–gel procedure given by Wang et al. [23] was modified in this study to prepare ZnO–SiO_2 catalysts in one pot synthesis approach. All chemicals were supplied by Sigma-Aldrich and Acro Inc. Briefly, tetraethyl orthosilicate (abbreviated as TEOS) (99.99%) was first diluted in ethanol (200 proof, 99.5%) and then the necessary amount of HCl (37%) was added. This was followed by adding necessary amount of water and heating the mixture to ~77 °C under total reflux. The mixture was kept at this temperature for 2 h. Finally, to obtain a gel, a necessary amount of ammonia solution (29.3% NH_3) was added to the mixture (TEOS:C_2H_5OH:HCl:H_2O:NH_4OH molar ratio was $1:22:7.9\times10^{-4}:13:2.5\times10^{-3}$) at ~77 °C. The difference between pure SiO_2 and ZnO/SiO_2 catalysts is the addition of zinc nitrate precursor ($Zn(NO_3)_2.6H_2O$ (98%) or $Zn(NO_3)_2.H_2O$ (99.999%)) before adding NH_4OH. Pure SiO_2 gel was obtained in ~10 min whereas ZnO/SiO_2 gels were formed in ~2 h. Finally, all the gels were dried at 120 °C for 24 h. Then, they were heated to 500 °C at a heating rate of 8 °C/min and once 500 °C was reached, they were kept at this temperature for 12 h.

In the preparation of pure ZnO, $Zn(NO_3)_2.6H_2O$ was precipitated by adding NH_4OH solution at room temperature and the solution pH was kept at ~10 for 1 h. After that, the precipitate was filtered and washed twice with room temperature de-ionized water and then twice with de-ionized water at 60°C. After that, the washed precipitate was vacuum

filtered. Finally, the same drying and calcination procedure used for the single step sol–gel made catalysts were also applied for the filtered precipitate.

2.2. Catalyst activity tests

It is known that during production of bio-ethanol from biomass, ethanol concentration in the aqueous solution ranges from 10% to 18%, which depends on the feedstock [24]. So, in this study, the molar ratio of water to ethanol was fixed at 12; hence simulating the bio-ethanol solution concentration. Also this ensures no carbon deposition on the catalysts for steady state runs as reported by others [19,20]. We did not observe any decrease in the conversion during the tests at each temperature and also the activity test was repeated on the same catalyst for a second day. We found that there was no change in the conversion within our experimental error; thus indicating no carbon deposition. But carbon deposition may occur on ZnO based catalysts especially when used under high ethanol concentration at high temperatures [21]. The premixed solution of de-ionized H_2O and C_2H_5OH was fed using a peristaltic pump into a Pyrex glass vaporizer at 145 °C. The vapor was then carried by argon gas to a straight downward Pyrex glass micro-reactor (I.D. 4 mm) through the heated lines at 145 °C. Argon and pump flow rates were adjusted to obtain a gas composition of 1% C_2H_5OH and 12% H_2O at the inlet of the catalyst bed. The catalyst inside the tube was held in place by glass wool plugs. The temperature of the catalyst was measured by a K-type thermocouple positioned in such a way that it touched the surface of the catalyst bed. In order to eliminate the catalytic effect of the thermocouple, the thermocouple was tightly inserted in a thin wall Pyrex glass tube. All the catalysts were ground and sieved to 100–120 mesh size prior to the activity tests. The temperature range from 300 to 500 °C with a 50 °C increment was used to evaluate the catalytic activity and selectivity of the catalysts. In all the tests, the gas hourly space velocity was kept at $\sim 42,000\,h^{-1}$ (0.03–0.15 g of catalyst).

In all the activity tests, the catalysts were heated to 500 °C under the flow of He and kept there for 1 h. Then it was cooled down in He to the reaction temperature and then the reactants were fed to the reactor. After reaching the steady state (it takes ~1 h) at each temperature, the reactor outlet was analyzed using an online Varian micro-GC CP4900 gas chromatography equipped with two TCD detectors. Molecular sieve and Porapak Q columns were used to separate the products for the analysis by the detectors. H_2, CO and CH_4 were separated in molecular sieve column using argon as the carrier gas whereas CO_2, C_2 compounds, C_3 compounds, C_2H_4O, $(CH_3)_2CO$ were separated in Porapak Q column using helium as the carrier. The calibration curves were prepared for each product by diluting standard gas mixtures (Cryogenic Co.) with pure He using calibrated mass flow controllers and volumetric gas flow meters. Under these conditions, the maximum experimental error based on 95% confidence interval was found to be ~4.5%. Since the micro-GC is very sensitive to water, the reactor outlet stream was dried using a membrane drier (from Perma Pure Inc.) to separate water. But it was found that most of ethanol was also removed with water. Therefore, the ethanol conversion and H_2 molar ratio are defined as

$$\text{Ethanol conversion}(\%) = \frac{\text{Total carbon in all products at the exit (mol/min)}}{\text{Carbon in ethanol feed (mol/min)}} \times 100,$$

$$H_2 \text{ molar ratio} = \frac{\text{Hydrogen produced (mol/min)}}{\text{Ethanol converted (mol/min)}}.$$

For acetaldehyde steam reforming, argon was purged through an acetaldehyde (99%) saturator at −35 °C and then entered the Pyrex glass vaporizer at 145 °C in order to mix with water pumped with the peristaltic pump. The molar concentration of water and acetaldehyde was adjusted with argon gas and pump flow rates to obtain 1% C_2H_4O and 12% H_2O in the gas before entering the reactor (in order to simulate the maximum concentrations obtained during ethanol steam reforming).

2.3. Catalyst characterizations

The crystalline phases present in all the calcined catalysts were determined by X-ray diffraction (XRD) (from Philips Inc., operated at 45 V and 40 A). The average crystallite sizes were calculated from X-ray line broadening using the Scherrer equation. The total surface areas of the catalysts were found by using Micromeritics 2010 adsorption equipment. Prior to the analysis, each sample was evacuated at 300 °C until the vacuum inside the sample tube stayed at 3 μm Hg or less. In addition, CO_2 TPD was performed to measure the basicity of all catalysts using Micromeritics AutoChem 2910 equipped with an inline Balzers Thermostar GS300 quadrupole mass spectrometer. 0.1 g of a catalyst was first degassed under He flow (20 cm^3/min) at 500 °C for 2 h and then cooled down to room temperature in He. CO_2 adsorption was done with 20 cm^3/min of pure CO_2 for 1 h at room temperature. After that, the catalyst was purged with helium for 1 h at room temperature to remove gas phase and weakly adsorbed CO_2. TPD was performed under He flow of 20 cm^3/min from room temperature to 500 °C at a heating rate of 10 °C/min.

3. Results

3.1. Catalyst characterizations

Fig. 1 shows the XRD spectra of ZnO/SiO_2 catalysts as a function of ZnO loading. As seen in the figure, over 50% ZnO/SiO_2 catalyst (the same XRD pattern obtained over 30% ZnO/SiO_2), there are no XRD peaks corresponding to ZnO crystalline phases. In contrast, the diffraction pattern of ZnO crystalline phase is clearly seen in 70% ZnO/SiO_2 catalyst. Since XRD analysis is sensitive to crystallite size greater than 5 nm, the average ZnO crystallite size in 30% ZnO/SiO_2 and 50% ZnO/SiO_2 catalysts are less than or equal to 5 nm whereas in 70% ZnO/SiO_2 catalyst, the average ZnO crystallite size calculated using Scherrer equation and the diffraction peak located at ~36° 2θ is ~19 nm. The XRD spectra of pure ZnO is also shown in Fig. 1 and similarly, the average ZnO crystallite size calculated using Scherrer equation and ~36° 2θ of the diffraction peak is ~37 nm. Also we found that the examination

of 50% ZnO with XRD after the activity test revealed no ZnO crystallite size increase.

Surface areas and pore volumes of all the catalysts are given in Table 1. As seen in the table, the sol–gel made catalysts have very high surface areas and total pore volume as compared to the precipitation made catalyst. The total surface area and the average pore size of pure SiO_2 catalyst are 887 m^2/g and ~2 nm, respectively. However, loading SiO_2 with 30 and 50 wt% ZnO decrease the surface area to 420 and 169 m^2/g, respectively. A further increase of the ZnO loading to 70 wt% decreases the surface to 112 m^2/g with the increase of the average pore diameter to ~6 nm. In contrast to the single step sol–gel made catalysts, the precipitation method results in pure ZnO catalyst with a small surface area, ~3 m^2/g, and the large pore diameter, 70 nm. The contribution of the micropores to total pore volume is less than 15% in all the catalysts. In fact, SiO_2 supported ZnO made using the single step sol–gel procedure actually decreases the sintering of ZnO during the heat treatment; hence resulting in the high surface area ZnO/SiO_2 catalysts.

Fig. 2 shows that 30% ZnO–SiO_2 catalyst adsorbs the highest amount of CO_2 whereas it stays the same over 70% and 50% ZnO. The low CO_2 adsorption is observed on pure SiO_2 and ZnO catalysts; in fact, the lowest on pure ZnO catalyst. The reason why pure SiO_2 shows higher total CO_2 adsorption than pure ZnO (although the catalyst amounts used in CO_2 TPD are the same as seen in Table 1) is as expected taking into account the specific surface areas of the catalysts. Hence, to eliminate the surface area effect, we calculated the basic site density (i.e. the amount of adsorbed CO_2 per surface area of the catalyst). We have found that pure ZnO being more basic than SiO_2 is in agreement with the literature [10]. The change of basic site density and the location of the peak temperature over all the catalysts as a function of ZnO loading are given in Table 2. The percent surface coverage of the basic sites was also calculated by using 1×10^{19} m^{-2} of surface sites. It is seen that the highest surface coverage of basic sites is 2.63% on pure ZnO and the lowest (~0.05%) on pure SiO_2. On the other hand, the surface coverage of basic sites on all ZnO/SiO_2 catalysts was found to be comparable.

3.2. *Activity and selectivity measurements*

3.2.1. *The catalytic reforming of bioethanol*

Fig. 3a shows the effect of ZnO loading on the ethanol conversion for all ZnO/SiO_2 catalysts and also the conversion

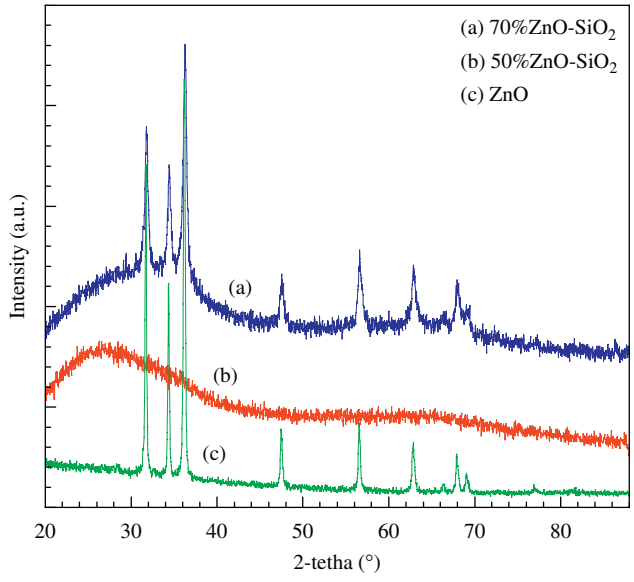

Fig. 1 – XRD spectra of ZnO/SiO_2 and pure SiO_2 catalysts as a function of ZnO loadings.

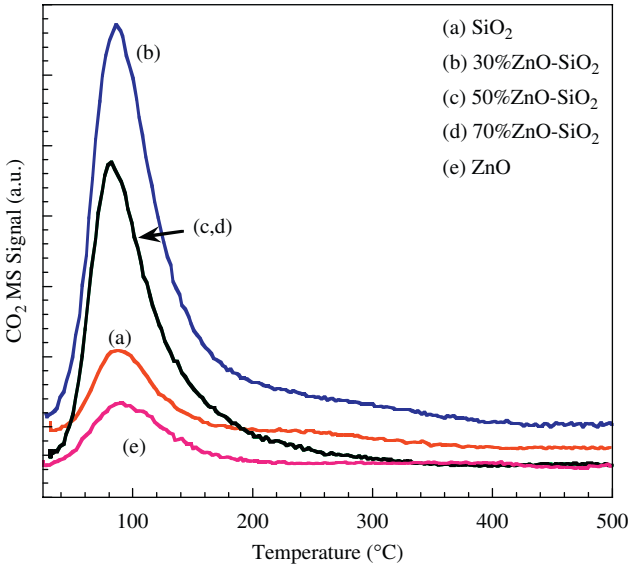

Fig. 2 – Temperature programmed desorption of CO_2 over all the catalysts.

Table 1 – BET surface areas and average pore diameters of all the catalysts

Catalysts	BET surface area (m^2/g)	Total pore volume (cm^3/g) (at $P/P_o = 0.95-0.97$)	Micropore volume (cm^3/g) from t-method	BET average pore diameter (nm)
SiO_2	887	0.5456	0.0502	2
30% ZnO–SiO_2	420	0.2208	0.0138	2
50% ZnO–SiO_2	169	0.1888	0.0021	4
70% ZnO–SiO_2	112	0.1796	0.0043	6
ZnO	~3	0.0039	0.0006	70

Table 2 – Base densities and peak temperatures for all the catalysts

	Adsorbed CO_2 ($\mu mol/m^2$)	Peak temperature (°C)	Surface coverage[a] (%)
Pure SiO_2	0.01	87	0.05
30% ZnO–SiO_2	0.02	87	0.12
50% ZnO–SiO_2	0.04	82	0.25
70% ZnO–SiO_2	0.05	82	0.32
Pure ZnO	0.44	88	2.63

[a] It is based on the surface site density of $1 \times 10^{19}\ m^{-2}$.

activities over the pure ZnO and SiO_2 catalysts as a function of temperature. Prior to testing the catalysts, we checked the reactor setup in the absence of a catalyst (with only glass wool plugs) for homogeneous reaction using the same inlet composition as given in Fig. 3a at 500 °C and found that there was no conversion under this reaction condition. As seen in Fig. 3a, pure SiO_2 is the least active among the other catalysts at all temperatures and pure ZnO catalyst is active above 400 °C. In contrast, all ZnO/SiO_2 catalysts are more active than both pure ZnO and SiO_2 catalysts. The lowest conversion (~5–10%) is obtained at 325 °C over ZnO/SiO_2 catalysts but as the temperature is increased to 400 °C, the ethanol conversion increases linearly with ZnO loading. Interestingly, we have found that ethanol conversions above 400 °C are similar over 50% and 70% ZnO catalysts within our experimental error whereas the conversion over 30% ZnO is still lower than others.

H_2 molar ratio as a function of temperature over ZnO/SiO_2 and pure ZnO catalysts is shown in Fig. 3b. H_2 molar ratio over 30%, 50% and 70% ZnO/SiO_2 catalysts are equal to 1 until 450 °C. At 500 °C, it increases to 1.1 over 30% and 50% ZnO/SiO_2 catalysts and ~1.2 over 70% ZnO/SiO_2 catalyst. In contrast, pure ZnO produces 20–30% more H_2 than that all ZnO/SiO_2 catalysts.

The product distributions in ethanol steam reforming are given in Table 3. H_2 and C_2H_4O are major products regardless of ZnO loading over all the catalysts. On 30% and 50% ZnO loadings, there is no formation of acetone at any temperature. But on 70% ZnO/SiO_2 and pure ZnO catalysts, acetone is produced at 450 °C and increases with the temperature. In addition, low percentages of C_2H_4, CO_2, C_3H_6 and CH_4 are produced on all catalysts at all temperatures. On ZnO/SiO_2 catalysts, C_2H_4 and CO_2 percentages increase with ZnO loading while C_3H_6 percentage stays constant while CH_4 percentage shows a minimum at 50% ZnO loading. Similar product distribution is observed on pure ZnO catalyst but acetone ($(CH_3)_2CO$) formation is much higher. As compared to ZnO/SiO_2 catalysts, C_3H_6 and CH_4 are produced in small amounts (<~0.3%) at all temperatures.

It is known that the selectivity is a function of conversion. Therefore, we changed the amount of catalysts and the flow

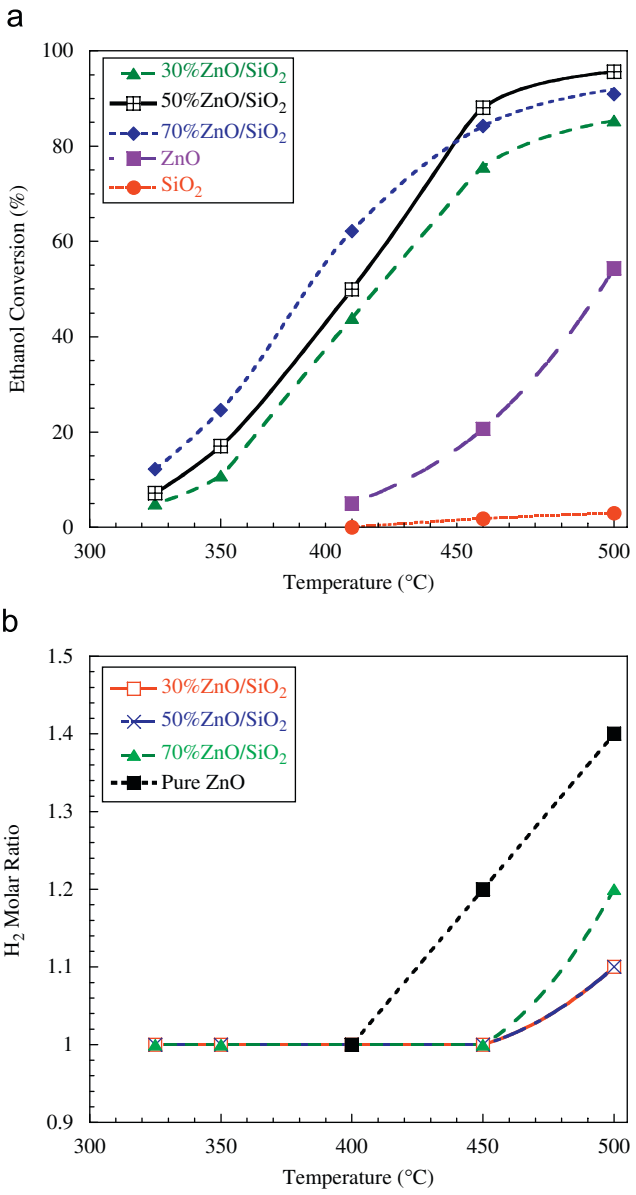

Fig. 3 – (a) The activities of all the ZnO/SiO_2 catalysts as a function of temperature. Reaction conditions: 1% ethanol, 12% water and argon being the balance. (b) H_2 molar ratio over all the ZnO/SiO_2 catalysts as a function of temperature. Reaction conditions are the same as (a).

rates in order to obtain the same conversions at a constant temperature under the same inlet condition and space velocity. A high conversion (~92%) was chosen because it was not possible to handle very high flow rates and large amounts of catalysts in our reactor setup to achieve a differential reactor regime. The results of iso-conversion tests for the ethanol steam reforming are given in Table 4. A temperature of 500 °C was chosen because it gave the highest acetone formation. Pure SiO_2 could not be used because it was not active. As seen in Table 4, on 30%, 70% ZnO and also pure ZnO catalysts, the formation of CO_2 increases as C_2H_4O amount decreases by producing more H_2. The

formations of C_3H_6 and CH_4 on 30% and 70% ZnO catalysts are higher than pure ZnO and 50% ZnO/SiO_2 catalysts.

3.2.2. The catalytic steam reforming of acetaldehyde

Acetaldehyde steam reforming at the same space velocity as used in ethanol steam reforming is shown in Fig. 4 as a function of ZnO loading and temperature. As seen in the figure, all the catalysts are active above 400 °C and their activities increase with the ZnO loading and the temperature. At 500 °C, acetaldehyde conversion is ~33% on pure ZnO, ~13% on 70% ZnO/SiO_2, 4% on 30% ZnO and 5% on 50% ZnO/SiO_2 catalysts, respectively. The product distribution is shown in Table 5. H_2 amount decreases while $(CH_3)_2CO$ amount increases with temperature on all the catalysts.

Iso-conversion activity tests for acetaldehyde steam reforming were also performed at 500 °C. The results are shown in Table 6. The amounts of H_2 and $(CH_3)_2CO$ increase with ZnO loading; reaching a maximum on pure ZnO catalyst as seen in the table. On the other hand, CH_4 and CO_2 amounts decrease with ZnO loading. CO and C_3H_6 amounts do not change significantly with ZnO loading.

4. Discussion

4.1. Activity and selectivity in catalytic reforming of bio-ethanol

The average specific rate (mmol ethanol/(m^2 of catalyst)/h) at 500 °C and ~92% of ethanol conversion is found to be 0.04, 0.101, 0.029 over 30%, 50% and 70% ZnO, respectively. Since the catalysts with 30% and 50% ZnO have crystals with sizes less than 5 nm, it is difficult to interpret the effect of the crystallite size and basic site density just by looking at 30 and 50% ZnO. To observe this crystallite size range, transmission electron microscopy (TEM) is needed to determine crystallite size distribution on 30 and 50% ZnO catalysts. Unfortunately, TEM is not available in our institute. However, still we can obtain some insight on the relationship between the

Table 3 – Dry product distribution (%) in ethanol steam reforming for all ZnO/SiO_2 and pure ZnO catalysts

°C	H_2	CH_4	CO	CO_2	C_2H_4	C_3H_6	C_2H_4O	$(CH_3)_2CO$
30% ZnO								
325	49.7	0.0	0.0	0.0	1.1	0.0	49.2	0.0
350	49.4	0.0	0.0	0.0	1.3	0.0	49.3	0.0
400	49.5	0.0	0.0	0.1	2.0	0.0	48.4	0.0
450	49.6	0.1	0.0	0.4	2.0	0.1	47.8	0.0
500	51.0	1.0	0.0	2.1	1.4	0.5	44.0	0.0
50% ZnO								
325	49.8	0.0	0.0	0.0	0.6	0.0	49.7	0.0
350	49.9	0.0	0.0	0.0	0.7	0.0	49.4	0.0
400	50.2	0.0	0.0	0.1	1.0	0.0	48.7	0.0
450	50.6	0.1	0.0	0.3	1.0	0.1	47.8	0.0
500	51.4	0.7	0.0	1.7	1.0	0.4	44.9	0.0
70% ZnO								
325	50.1	0.0	0.0	0.0	0.4	0.0	49.5	0.0
1350	49.8	0.0	0.0	0.0	0.5	0.0	49.7	0.0
400	50.1	0.0	0.0	0.2	0.6	0.0	49.1	0.0
450	50.8	0.2	0.0	0.8	0.6	0.2	47.4	0.1
500	53.0	2.0	0.0	4.0	0.4	0.5	39.2	0.7
Pure ZnO								
400	50.8	0.0	0.0	1.5	2.3	0.0	45.4	0.0
450	52.5	0.2	0.0	3.1	2.9	0.0	39.7	1.5
500	57.5	0.3	0.0	8.8	2.4	0.2	25.0	5.8

Reaction conditions are given in Fig. 3a.

Table 4 – Dry product distribution (%) at 500 °C and a constant ethanol conversion in ethanol steam reforming

	Ethanol conversion	H_2	CH_4	CO	CO_2	C_2H_4	C_3H_6	C_2H_4O	$(CH_3)_2CO$
30% ZnO–SiO_2	91.8	57.0	5.44	0.0	9.2	0.8	1.2	26.4	0.0
50% ZnO–SiO_2	92.0	51.4	0.7	0.0	1.7	1.0	0.4	44.9	0.0
70% ZnO–SiO_2	92.3	61.0	7.8	0.0	12.7	0.3	1.1	15.2	2.0
Pure ZnO	91.7	58.6	0.4	0.0	9.5	1.6	0.3	22.1	7.6

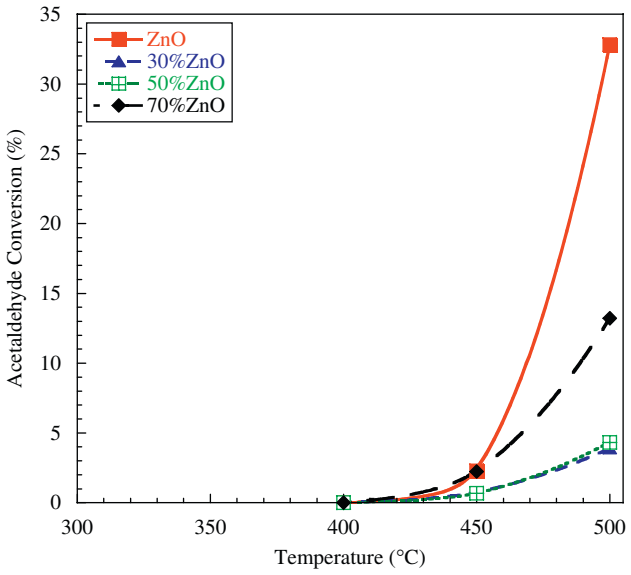

Fig. 4 – The activities of all the ZnO/SiO_2 catalysts and pure ZnO catalyst as a function of temperature. Reaction conditions: 1% acetaldehyde, 12% water and argon being the balance.

Table 5 – Dry product distribution (%) in acetaldehyde steam reforming for all ZnO/SiO_2 and pure ZnO catalysts

°C	H_2	CH_4	CO	CO_2	C_3H_6	$(CH_3)_2CO$
30% ZnO						
400	0.0	0.0	0.0	0.0	0.0	0.0
450	59.1	8.2	0.0	24.7	8.0	0.0
500	44.8	17.2	1.7	30.6	5.7	0.0
50% ZnO						
400	0.0	0.0	0.0	0.0	0.0	0.0
450	50.2	7.4	0.0	30.9	11.4	0.0
500	46.2	14.9	2.9	29.1	5.3	1.5
70% ZnO						
400	0.0	0.0	0.0	0.0	0.0	0.0
450	72.0	5.5	0.0	16.1	4.0	2.4
500	50.4	15.4	0.7	25.8	3.2	4.5
Pure ZnO						
400	0.0	0.0	0.0	0.0	0.0	0.0
450	67.5	1.8	2.3	19.8	0.0	8.6
500	52.7	1.5	0.9	25.7	1.1	18.1

Reaction conditions are the same as that given in Fig. 4.

crystallite size and basic site density using 50 and 70% ZnO/SiO_2 and pure ZnO catalysts. The specific rate decreases from 0.101 to 0.029 when ZnO loading is increased from 50% to 70%. The rate obtained over 70% ZnO is ~3.5 times less than that of 50% ZnO. If we look at the crystallite size change with the ZnO loading, we see that ZnO crystallite size on 70% ZnO is 3.8 times larger than that of 50% ZnO. In contrast, the basic site density of 70% ZnO is only 25% higher than 50% ZnO and also the basic site density surface coverage of all the catalysts is $\leqslant$0.32%. Interestingly, this indicates that the rate changes almost linearly with the crystallite size rather than the basic site density of the ZnO/SiO_2 catalysts. However, when pure ZnO is compared to 50% and 70% ZnO, it is seen that pure ZnO shows the highest specific rate of 1.603 mmol ethanol/(m^2 of catalyst)/h at 500 °C and ~92% ethanol conversion. The specific rate obtained over pure ZnO is ~15 times higher than 50% ZnO catalyst. The crystallite size of pure ZnO is 2.1 times larger than ZnO crystals found in 50% ZnO catalyst and the basic site density of pure ZnO is ~11 times higher than 50% ZnO. Comparison of 50% and 70% ZnO/SiO_2 catalysts to pure ZnO catalyst indicates that when the surface coverage of the basic site density (given in Table 2) is >0.32%, the rate is strongly influenced by the basic site density of the catalyst but the crystallite size effect still cannot be ignored.

In the literature, there is no study on the effect of ZnO crystallite size and/or ZnO basic site density on the activity and the product distribution of ZnO based catalysts for the steam reforming of ethanol. It is not easy to compare results reported by laboratories around the world because inlet compositions, conversions, space velocities and temperatures are different. For example, Guil et al. [29] reported that the rate of ethanol consumption over pure ZnO catalyst (operated under 10,000 h^{-1} GHSV and H_2O/C_2H_5OH ratio of 3) was 0.85 mmol ethanol/(g of catalyst)/h at 450 °C. Since their ZnO catalyst had a surface area of 100 m^2/g, the specific rate of ethanol consumption could be calculated as 0.85×10^{-2} mmol ethanol/(m^2 of catalyst)/h. This specific rate is almost 2 orders of magnitude lower than the specific rate obtained over our pure ZnO catalyst but it should be noted that their temperature was 450 °C and also water-to-ethanol ratio was 3.

For ZnO based catalysts, Llorca et al. [20] was the first group to report the effect of the precursor used to prepare ZnO on the product distribution without giving experimental finding but they only claimed that the formation of acetone and acetaldehyde was through dehydrogenation of ethanol and the aldol condensation and redox capabilities of ZnO

Table 6 – Dry product distribution (%) at 500 °C and a constant acetaldehyde conversion in acetaldehyde steam reforming over all the catalysts

	Acetaldehyde conversion	H_2	CH_4	CO	CO_2	C_3H_6	$(CH_3)_2CO$
30% ZnO	4.4	44.8	17.2	1.7	30.6	5.7	0.0
50% ZnO	5.1	46.3	14.9	2.9	29.1	5.3	1.5
70% ZnO	4.5	48.6	9.2	2.8	28.2	6.9	4.3
Pure ZnO	4.2	55.4	3.0	2.7	25.1	0.7	13.2

catalysts. The product distribution obtained over ZnO/SiO_2 in this manuscript is similar to those reported by others [20,29]. But we show that although 30%, 50% and 70% ZnO/SiO_2 and also pure ZnO catalysts are basic (with varying amounts), the rate of acetaldehyde consumption during ethanol steam reforming seems to be mainly affected. It is known that dehydrogenation of ethanol occurs on the basic catalysts [10]. It is not easy to distinguish the crystallite size effect from the basic site density on the conversion of acetaldehyde but the main difference between the catalysts is the formation of acetone which results from the aldol reactions as shown below [25]:

$$2C_2H_5OH + H_2O \leftrightarrow (CH_3)_2CO + CO_2 + 4H_2. \quad (7)$$

The basic site density of 50% ZnO is twice that of 30% ZnO (both with less than 5 nm ZnO crystallite size) and also the basic site density over 70% ZnO catalyst (with ~19 nm ZnO crystallite size) increases only 25% as compared to that of 50% ZnO catalyst. Although 30%, 50% and 70% ZnO/SiO_2 catalysts are basic (with varying amounts), $(CH_3)_2CO$ formation occurs only on 70% ZnO/SiO_2 catalyst. So, it seems that when ZnO crystallite size <5 nm, $(CH_3)_2CO$ is not produced during ethanol steam reforming. However, it is not easy to separate the effect of the crystallite size from the basic site density on the formation of acetone when the crystallite sizes are >5 nm as seen over 70% ZnO and pure ZnO catalyst. Unfortunately, we cannot control the size of the ZnO on ZnO/SiO_2 catalysts by using single step sol–gel method when the ZnO loading is above 70%. The work on controlling ZnO crystals between 19 and 40 nm for ZnO/SiO_2 catalysts is in progress.

4.2. *Activity and selectivity in steam reforming of acetaldehyde*

The rate (mmol acetaldehyde/h/(m^2 of catalyst)) of acetaldehyde consumption in the steam reforming of acetaldehyde increases with ZnO loading over ZnO/SiO_2 and reaches a maximum over pure ZnO catalyst; 0.0017, 0.0043, 0.0106 and 0.6436 over 30%, 50%, 70% ZnO/SiO_2 and pure ZnO, respectively. The basic site density doubles when ZnO increases from 30% to 50% and also, the rate almost doubles. However, acetaldehyde consumption rate over 70% ZnO is 2.5 times higher than that of 50% ZnO while the basic site density increases only 25% and ZnO crystallite size quadruples when ZnO loading increases from 50% to 70%. These indicate that acetaldehyde steam reforming seems to be influenced by both ZnO crystallite size and the basic site density.

We have also found that C_3H_6 and $(CH_3)_2CO$ are produced from acetaldehyde during the steam reforming of ethanol through the following possible reactions, as suggested in Refs. [26–28]:

$$2C_2H_4O + H_2O \rightarrow (CH_3)_2CO + CO_2 + 2H_2, \quad (8)$$

$$2C_2H_4O \rightarrow C_3H_6 + CO_2 + H_2. \quad (9)$$

It seems that the production of C_3H_6 is dependent on basic site density of the catalyst rather than the ZnO crystallite size as seen in Table 6. Its formation is favored at low basic site densities ($<0.05\,\mu mol/m^2$) regardless of ZnO crystallite size. In addition, CO was found to form over all the catalysts regardless of ZnO loading and the basic site density. However, the production of CH_4 decreases from 30% ZnO/SiO_2 to pure ZnO. Since CH_4 formation could occur through the possible reactions [26,27], it seems that acetaldehyde steam reforming (reaction 10) occurs more over 30% and 50% ZnO catalysts.

$$C_2H_4O + H_2O \rightarrow CH_4 + CO_2 + H_2, \quad (10)$$

$$C_2H_4O \rightarrow CH_4 + CO. \quad (11)$$

Our results show that the decomposition of acetaldehyde (reaction 11) occurs mainly on pure ZnO since CH_4/CO ratio in the product stream is almost one. Whereas, over ZnO/SiO_2 catalysts, steam reforming of acetaldehyde (reaction 10) seems to occur faster than the decomposition of acetaldehyde (reaction 11). This indicates that the acetaldehyde steam reforming is favorable over the catalysts with small ZnO crystals, such as 30% and 50% ZnO. Similar observations and explanations were also suggested by others [20,29]. Also we have found that there is no $(CH_3)_2CO$ formation in ethanol steam reforming over 50% ZnO catalyst whereas it is produced during acetaldehyde steam reforming. This may be due to the adsorption of ethanol on possible active site(s) responsible for acetaldehyde steam reforming; hence blocking the formation of $(CH_3)_2CO$ during ethanol steam reforming.

5. Conclusion

In this study, we show that the small ZnO crystallite size in SiO_2 could be prepared with the modified single step sol–gel method but the fine tuning of crystallite size could not be achieved. Ethanol steam reforming activities over all catalysts are found to be dependent on the surface coverage of basic site density. When it is $<0.32\%$, the rate changes almost linearly with the crystallite size but when the surface coverage is $>0.32\%$, both crystallite size and basic site density affect the steam reforming activity. In contrast, acetone during ethanol steam reforming is not formed when crystallite size is <5 nm. Also, we have found that although H_2O/C_2H_5OH molar ratio used in this study was 12, the dehydrogenation of ethanol still occurs on all the catalysts; hence giving hydrogen molar ratio between 1 and 2. CO formation during ethanol steam reforming is not observed on any of the catalysts at any temperature; hence indicating that no decomposition reaction occurs.

The steam reforming of acetaldehyde shows that the steam reforming reaction is more favorable as compared to the decomposition over the catalysts with small ZnO crystals. Both ZnO crystallite size and the basic site density affect the rate of acetaldehyde consumption and also acetone formation. However, C_3H_6 formation is dependent on the basic site density of the catalysts rather than their ZnO crystallite size.

Acknowledgments

We would like to greatly thank Prof. Erdogan Gulari of the Chemical Engineering Department at the University of Michigan for the use of his laboratory for some of the experiments and also the Scientific & Technological Research

Council of Turkey (TUBITAK) for the financial support through the project code of MISAG 241. The help of Timothy E. King in collecting CO_2 TPD data in the Chemical Engineering Department at the University of Michigan is appreciated.

REFERENCES

[1] United States Environmental Protection Agency EPA-456/F-98-005, September 1998.
[2] Creveling HF. In: Proceedings of the annual automotive technology development contractors' coordination meeting. October 1992: Society of Automotive Engineers; 19–21. pp. 485–492.
[3] The US Energy Policy Act Fleet Requirements, Public Law 102-486, October 24 1992.
[4] Kobayashi H, Takezawa N, Minochi CJ. Catal 1981;69(2):487.
[5] Takahashi K, Takezawa N, Kobayashi H. Appl Catal 1982; 2:363.
[6] Rostrup-Nielsen JR. Phys Chem Chem Phys 2001;3:283–8.
[7] Vasudeva K, Mitra N, Umasankar P, Dhingra SC. Int J Hydrogen Energy 1996;21:13–8.
[8] Ioannides T. J Power Sources 2001;92:17–25.
[9] Fishtik I, Alexander A, Datta R, Geana D. Int J Hydrogen Energy 2000;25:31–45.
[10] Tanabe K. Solid acids and bases; their catalytic properties. Tokyo: Academic Press; 1970.
[11] Takezawa N, Hanamaki C, Kobayashi HJ. Catal 1975;38:101–9.
[12] Fumihiro H, Tsuyoshi N, Hidemaru M, Shozi M. Catal Lett 1997;48:223.
[13] Cavallaro S. Energy Fuels 2000;14:1195–9.
[14] Comas J, Marino F, Laborde M, Amadeo N. Chem Eng J 2004;98:61.
[15] Fatsikostas NA, Verykios XE. J Catal 2004;225:439–52.
[16] Zhang B, Tang X, Li Y, Cai W, Xu Y, Shen W. Catal Commun 2006;7:367.
[17] Kugai J, Velu S, Song C. Catal Lett 2005;101(3–4):255.
[18] Barroso MN, Gomez MF, Arrua LA, Abello MC. Catal Lett 2006;109(1–2):13.
[19] Benito M, Sanz JL, Isabel R, Padilla R, Arjona R, Daza LJ. Power Sources 2005;151:11.
[20] Llorca J, Piscina PR, Sales J, Homs N. Chem Commun 2001:641–2.
[21] Llorca J, Homs N, Sales J, Piscina PR. J Catal 2002;209: 306–17.
[22] Yang Y, Ma J, Wu F. Int J Hydrogen Energy 2006;31:877.
[23] Wang D, Luo H, Kou R, Gil MP, Xiao S, Golub VO, et al. Chem Int Ed 2004;43:6169–73.
[24] Minter S. Alcoholic fuels. Boca Raton: Taylor & Francis; 2006.
[25] Nishiguchi T, Matsumoto T, Kanai H, Utani K, Matsumura Y, Shen WJ, et al. Appl Catal A Gen 2005;279:273–7.
[26] Idriss H, Diagne C, Hindermann JP, Kiennemann A, Barteau MA. J Catal 1995;155:219–37.
[27] Kiennemann A, Idriss H, Kieffer R, Chaumette P, Durand D. Ind Eng Chem Res 1991;20:1130–8.
[28] Alkhazov TG, Adzhamov KY, Khanmamedova AKK. Russ Chem Rev 1982;51(6):542–51.
[29] Guil JM, Homs N, Llorca J, Piscina PR. J Phys Chem B 2005; 109:10813–9.